Eur Biophys J (2002) 31: 185–197
DOI 10.1007/s00249-002-0211-9

ARTICLE

**Béatrice de Foresta · Ludovic Tortech · Michel Vincent
Jacques Gallay**

Location and dynamics of tryptophan in transmembrane α-helix peptides: a fluorescence and circular dichroism study

Received: 28 September 2001 / Revised: 18 January 2002 / Accepted: 18 January 2002 / Published online: 8 March 2002

Abstract Amphiphilic and hydrophobic peptides play a key role in many biological processes. We have developed a reference system for evaluating the insertion of such peptides bearing Trp fluorescent reporter groups into membrane mimetic systems. This system involves a set of six 25-amino acid synthetic peptides that are models of transmembrane α-helices. They are Lys-flanked polyLeu sequences, each containing a single Trp residue at a different position (P*i*, with $i = 3$, 5, 7, 9, 11 and 13). These peptides were inserted into micelles of a non-ionic detergent, dodecylmaltoside (DM). We analyzed this system by use of circular dichroism and steady-state and time-resolved fluorescence in combination with Trp quenching with two brominated DM analogs. We found significant variations in the Trp emission maximum according to its position in each peptide (from 327 to 313 nm). This is consistent with the radial insertion of the peptides within DM micelles. We observed characteristic patterns of fluorescence quenching of these peptides in mixed micelles of DM, with either 7,8-dibromododecylmaltoside (BrDM) or 10,11-dibromoundecanoylmaltoside (BrUM), that reflect differences in the accessibility of the Trp residue to the bromine atoms located on the detergent acyl chain. In the isotropic reference solvent, methanol, the α-helix content was high and identical (~76%) for all peptides. In DM micelles, the α-helix content for P9 to P13 was similar to that in methanol, but slightly lower for P3 to P7. The fluorescence intensity decays were heterogeneous and depended upon the position of the Trp. The Trp dynamics of each peptide are described by sub-nanosecond and nanosecond rotational motions that were significantly lower than those observed in methanol. These results, which precisely describe structural, dynamic and microenvironment parameters of peptide Trp in micelles according to its depth, should be useful for describing the interactions of peptides of biological interest with micelles.

Keywords Fluorescent model polypeptides · Dodecylmaltoside · Brominated detergent · Steady-state and time-resolved fluorescence · Circular dichroism

Abbreviations *BrDM*: 7,8-dibromododecylmaltoside · *BrUM*: 10,11-dibromoundecanoylmaltoside · *CD*: circular dichroism · *DM*: dodecylmaltoside · *DPC*: dodecylphosphocholine · *DSC*: differential scanning calorimetry · *FTIR*: Fourier transform infrared spectroscopy · *MALDI/TOF*: matrix-assisted laser desorption ionization time-of-flight · *MEM*: maximum entropy method · *NATA*: *N*-acetyltryptophanamide · *SDS*: sodium dodecyl sulfate · *TOE*: tryptophan octyl ester · *C18:1PC*: dioleoylphosphatidylcholine · *P3*: $K_2WL_9AL_9K_2A$ · *P5*: $K_2CLWL_7AL_9K_2A$ · *P7*: $K_2CL_3WL_5AL_9K_2A$ · *P9*: $K_2CL_5WL_3AL_9K_2A$ · *P11*: $K_2CL_7WLAL_9K_2A$ · *P13*: $K_2CL_9WL_9K_2A$

Introduction

Understanding the interactions between peptides and membranes is an important issue because such interactions are implied in many biological processes. Membrane-active peptides include hormones, toxins and antimicrobial peptides (see Epand and Vogel 1999; Gao and Wong 1999; Lewis et al. 1999 for recent studies). Another case in which peptide-membrane interactions play an important role concerns the insertion of membrane proteins into lipid bilayers. It has been suggested that transmembrane fragments acquire their structure

B. de Foresta (✉) · L. Tortech
Section de Biophysique des Protéines et des Membranes,
Département de Biologie Cellulaire et Moléculaire
et URA 2096 (CNRS), CEA Saclay,
91191 Gif-sur-Yvette Cedex, France
E-mail: foresta@dsvidf.cea.fr
Tel.: +33-1-69088944
Fax: +33-1-69088139

M. Vincent · J. Gallay
LURE (Laboratoire pour l'Utilisation
du Rayonnement Electromagnétique),
Université Paris-Sud, Bât. 209D,
BP 34, 91898 Orsay Cedex, France

independently from one another before associating to form the transmembrane sectors of a protein (Popot and Engelman 1990). This hypothesis has already gained experimental support and justifies the study of isolated transmembrane segments (e.g. Katragadda et al. 2001 and references therein).

The mechanism of peptide-membrane interactions involves a succession of different steps which, in some cases, have been described as adsorption and structuring of the soluble random-coil peptide in an α-helical form at the membrane surface, followed by insertion of the helix into the membrane and association with other peptides to yield the active membrane form (Schwyzer 1995; Shepherd et al. 2001). The study of these events requires the development of specific techniques that differ from the conventional ones used in homogeneous solutions because they imply localized interactions at interfaces, inhomogeneous systems and, in addition, rapid transient phenomena.

Micellar systems are often used as membrane mimetic systems for different purposes such as to maintain membrane proteins in solubilized forms after their extraction from the membranes or for modeling protein- or peptide-membrane interactions. They have the advantage of possessing smaller sizes and low light-scattering levels, allowing optical and NMR techniques to be more easily applied than in lipid bilayers. We have developed the use of brominated detergents (de Foresta et al. 1996, 1999; Soulié et al. 1998), which allow the detection of Trp-detergent contacts from fluorescence quenching experiments and as a consequence may be of value for the study of peptide-detergent interactions. This type of approach has already been applied to the study of Ca^{2+}-ATPase transmembrane segments, M6 and M7 (Soulié et al. 1998). However, to interpret the data completely, a reference system with which to compare the data obtained on peptides of unknown insertion in the micelles seems to be necessary.

The purpose of our study was to use spectroscopic techniques (fluorescence and circular dichroism) to characterize such a reference system. It is constituted of a set of six synthetic Lys-flanked polyLeu peptides inserted in the micelles of a non-ionic detergent, dodecylmaltoside (DM). Each of the peptides contains a unique Trp at a different position. They were initially synthesized for hydrophobic mismatch studies (Ren et al. 1997). The Lys-flanked polyLeu peptides alone (with no Trp) have been studied as models of transmembrane helices by various techniques such as Fourier transform infrared spectroscopy (FTIR), differential scanning calorimetry (DSC) and circular dichroism (CD) (Davis et al. 1983; Huschilt et al. 1989; Zhang et al. 1992a, 1992b). Molecular dynamics studies have also been performed on such peptides (Belohorcová et al. 1997).

Here, fluorescence emission spectra and time-resolved fluorescence intensity and anisotropy decays of the Trp-containing peptides were measured, as were their quenching characteristics by two brominated analogs of DM, 7,8-dibromododecylmaltoside (BrDM) and 10,11-dibromoundecanoylmaltoside (BrUM). The secondary structure of these peptides was evaluated by CD. Our results allowed us to propose transmicellar insertion of this set of model peptides in DM micelles and to characterize variations in different parameters correlated with Trp depth in the micelle, such as the maximum emission wavelength (λ_{max}) and fluorescence quenching characteristics. They also emphasized the position-dependent constraints imposed by the micellar environment on peptide structure and dynamics.

Materials and methods

Materials

The six synthetic peptides $K_2WL_9AL_9K_2A$ (P3), $K_2CLWL_7AL_9K_2A$ (P5), $K_2CL_3WL_5AL_9K_2A$ (P7), $K_2CL_5WL_3AL_9K_2A$ (P9), $K_2CL_7WLAL_9K_2A$ (P11) and $K_2CL_9WL_9K_2A$ (P13), called P*i*, the index *i* denoting the Trp position, were purchased from Research Genetics (Huntsville, Ala., USA). The peptides all had acetylated N-termini and amide-blocked C-termini. Their purity was checked by matrix-assisted laser desorption ionization time-of-flight (MALDI/TOF) mass spectrometry by Research Genetics and they were used as supplied.

DM was obtained from Calbiochem and its brominated derivatives, BrDM and BrUM, were synthesized as previously described (de Foresta et al. 1996, 1999). *N*-Acetyltryptophanamide (NATA) was purchased from Sigma-Aldrich. Methanol and ethanol were from Merck (uvasol quality).

Water was first distilled and then purified by a Milli-Q system. All buffers were filtered through Millex-HA filters (0.45 μM pore size) (from Millipore).

Absorption measurements

Absorption spectra were recorded either on an HP 8452A or HP8453 diode array spectrophotometer, with a thermostatically controlled sample holder (20 °C). The sample was continuously stirred. The pathlength through the cuvette was 1 cm.

Steady-state fluorescence measurements

Fluorescence intensities were measured on a Spex Fluorolog spectrofluorometer. The temperature in the cuvette was controlled with a thermostat and the sample was continuously stirred. We used a standard quartz cuvette (1×1 cm). Excitation spectra were corrected for the spectrum of the lamp and both excitation and emission spectra were corrected for the fluctuations in lamp intensity (usually very low, $< 1\%$).

Time-resolved fluorescence measurements

Fluorescence intensity and anisotropy decays were determined by the time-correlated single-photon counting technique from the polarized components, $I_{vv}(t)$ and $I_{vh}(t)$, on the experimental setup of the SB1 window of the synchrotron radiation machine Super-ACO (Anneau de Collision d'Orsay), as previously described (Rouvière et al. 1997 and references therein). The excitation and emission wavelengths were respectively selected by use of a double (Jobin Yvon UV-DH10) and single monochromator (Jobin Yvon UV-H10). A Hamamatsu MCP-PMT (model R3809U-02) was used as detector. The time resolution was about 20 ps and the data were accumulated in 2048 channels. Automatic sampling cycles were carried out, including a 30 s accumulation time for the instrument response function and a 90 s acquisition time for each polarized component, so that a total of $(2–4)\times10^6$ counts was reached for each fluorescence intensity decay. Fluorescence

intensity and anisotropy decays, respectively $I(t)$ and $A(t)$, were analyzed as sums of 150 exponential terms by the maximum entropy method (MEM) (Livesey and Brochon 1987) according to:

$$I(t) = \sum \alpha_i \exp(-t/\tau_i) \quad (1)$$

where α_i is the normalized amplitude and τ_i the lifetime of the intensity decay, and:

$$A(t) = \sum \beta_i \exp(-t/\theta_i) \quad (2)$$

where β_i is the anisotropy and θ_i the rotational correlation time of the anisotropy decay. In this latter analysis, we assume that each lifetime τ_i is associated with all rotational correlation times θ_i.

We can recall that MEM imposes no a priori number of significant parameters of the decay. To ensure that the recovered distribution agrees with the data, the Skilling-Jaynes entropy S is subjected to a χ^2 constraint (Brochon 1994).

Circular dichroism

CD spectra were recorded on a Jobin Yvon CD6 spectrodichrograph, using a 1 mm pathlength quartz cuvette, at 20 °C. The spectral bandwidth was 2 nm, the wavelength increment and integration time were 0.5 nm and 2 s/step, respectively. Each spectrum resulted from the average of five successive individual spectra. Background spectra of the corresponding solvent (methanol or phosphate buffer plus detergent) were recorded under identical conditions and subtracted. Peptide concentration is indicated in the figure legends.

The α-helical content of the peptides was estimated from the ratio of the molar ellipticity value at 222 nm, $[\theta]_{222}$, to that characteristic of a 100% α-helix of same length, i.e. $[\theta]^{\infty}_{H,222}(1–k_{222}/n')$, where $[\theta]^{\infty}_{H,222}$ is the molar ellipticity at 222 nm of a helix of infinite length (i.e. –39,500 deg cm^2 dmol^{-1}), k_{222} is the chain-length-dependent factor at 222 nm (i.e. 2.57) and n' is the number of amino acid residues in the helix (Chen et al. 1974). In our conditions, n' varies between 14 and 20 (see Results).

Analysis of the fluorescence quenching data

To analyze fluorescence quenching of the various peptides in mixed micelles of DM with a brominated analog, we used the quenching model first described by London and Feigenson (1981) and used by East and Lee (1982); this model was originally designed to describe the quenching of membrane fluorophores (e.g. protein Trp) by spin-labeled or brominated phospholipids. This model considers two populations of fluorophores: one completely inaccessible to the quencher and responsible for the residual fluorescence F_{min} (e.g. Trp embedded in a protein), and another one in which each fluorophore has n neighbors (phospholipids) and the fluorescence of which is completely quenched if one (or more) of these sites is occupied by a modified phospholipid. Phospholipids are supposed not to change positions during the lifetime of the fluorophore. If X is the molar fraction of quenchers in the membrane, $(1–X)^n$ is the probability that none of the n sites is occupied by a quencher. The fluorescence ratio is therefore given by: $F/F_0 = (1 - F_{min}/F_0)(1 - X)^n + F_{min}/F_0$. We have previously discussed the application of this model for the quenching of a model compound, tryptophan octyl ester (TOE), by a brominated detergent in a micellar system (de Foresta et al. 1999); owing to the occurrence of some dynamic quenching (in addition to static quenching), as shown by TOE lifetime measurements, and to both lateral and transversal inaccessibility of the fluorophore, n is not expected to give an exact determination of quenchers around the fluorophore but is nevertheless correlated to the accessiblity of fluorophore to the brominated alkyl chains.

Solubilization assays of the peptides

Stock solutions (1 mM) of the peptides were prepared in methanol (this was done by weighing the appropriate amount of the lyophilized peptides and adding methanol, usually ~5 mg of peptides for 2 mL of methanol). All the peptides were readily soluble under these conditions. Absorption spectra were determined at a peptide concentration of 20 μM in methanol. All the peptide spectra were quite similar and characteristic of Trp absorption: they showed a main peak at 282 nm and a well-resolved shoulder at 290–291 nm. Attempts to solubilize the peptides in buffer with detergent concentrations corresponding to less than one detergent micelle per peptide (e.g. 1 mM peptide with 4 mM or 40 mM DM in 10 mM phosphate buffer, pH 7.5) resulted in progressive aggregation and precipitation of the peptides.

Preparation of the peptide-detergent complexes

The peptide-detergent complexes were obtained by adding a small aliquot of the peptide stock solutions (so that final peptide concentrations were 5–25 μM) to the appropriate buffer already containing an excess of detergent (usually 4 mM) (see figure legends). This was performed either directly in the fluorescence cuvette (with magnetic stirring) or in a 5 mL hemolysis tube (with vortexing), before transfer to the CD cuvette. About 2–3 min of equilibration were sufficient to obtain stable signals.

Results

Steady-state emission spectra of the model peptides in DM micelles

Figure 1 shows the excitation and emission spectra of P13 in DM micelles together with the emission spectra obtained in methanol and in buffer alone. P13 is the peptide for which the shifts in the emission spectrum from one medium to another were the greatest. Thus, the emission maximum for P13 changed from 338 nm in methanol to 332 nm in buffer and 313 nm in DM micelles, reflecting a large decrease in the polarity of the Trp environment. The emission spectra for all six peptides were recorded under the same conditions and the variations in the wavelengths of the emission maxima (λ_{max}) with the Trp position are plotted in Fig. 2. The emission maxima were nearly constant for the six peptides in methanol (337 ± 1 nm), reflecting a similar polarity in the environment of the Trp, which is probably largely exposed to the solvent. In contrast, significant emission maxima variations were observed for the peptides solubilized with micellar DM, with a plateau at ~327 nm for the peptides when Trp was near to the peptide N-terminus (P3, P5 and P7), followed by a regular decrease down to 313 nm from P7 to P13. Even for P3, P5 and P7, the Trp environment appeared to be less polar than in methanol. In buffer alone, a slight variation in the emission maxima was also observed, probably linked to the presence of a slight polarity gradient within the peptide aggregates under these conditions.

Time-resolved fluorescence intensity decays of the model peptides in methanol and in DM micelles

In methanol, at constant emission wavelength (338 nm), the fluorescence emission decays of the various peptides were heterogeneous, with two (for P3 and, in some

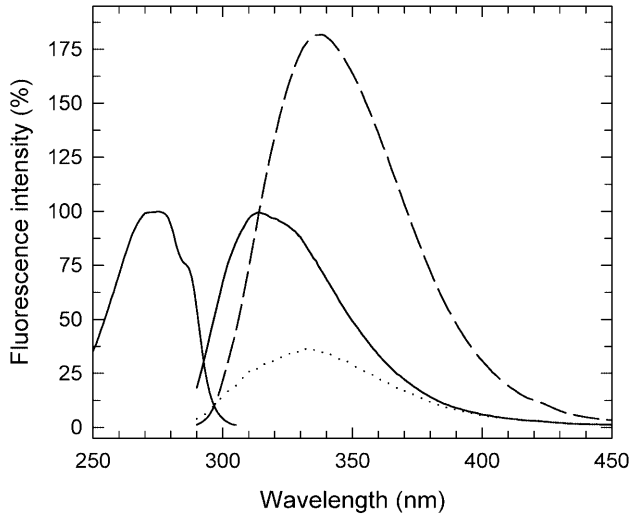

Fig. 1 Fluorescence excitation and emission spectra of P13 in DM micelles (*solid lines*). Comparison with emission spectra of P13 in methanol (*dashed line*) and in buffer (*dotted line*). Normalized excitation (*left*) and emission (*right*) spectra of P13 (5 μM) in 10 mM potassium phosphate buffer (K_2HPO_4/KH_2PO_4, pH 7.5) containing 4 mM DM (*solid lines*). For the excitation spectrum, λ_{em} was 312 nm, and for emission spectrum, λ_{ex} was 280 nm. *Dashed line*: emission spectrum of P13 (performed at 10 μM and normalized) in methanol, $\lambda_{ex} = 280$ nm. *Dotted line*: emission spectrum of P13 (5 μM) in buffer alone, $\lambda_{ex} = 280$ nm. In all cases, slit widths were 1.25 mm (bandwidths≈5 nm) at both excitation and emission. The spectra were recorded after 3 min equilibration. In buffer, the fluorescence decreased with time and under these conditions the fluorescence intensity was about 70% of its initial value. In buffer and in methanol, the fluorescence intensity is given as percentage of that obtained in buffer containing DM for the same peptide concentration. In all cases, blank spectra were subtracted. The temperature was 20 °C

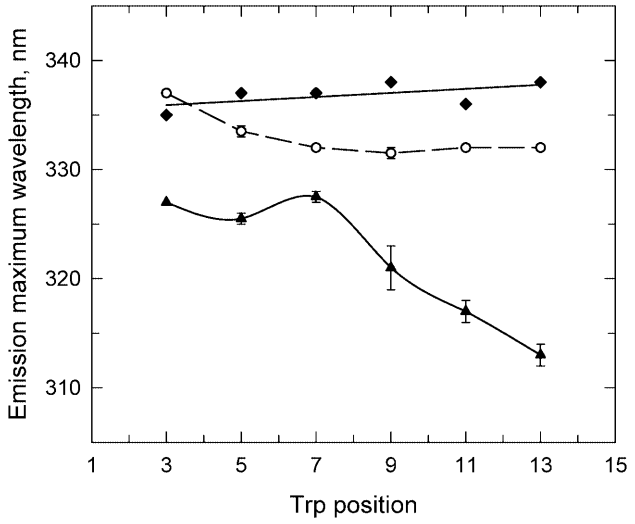

Fig. 2 Effect of Trp position on the fluorescence emission maximum wavelength (λ_{max}) of the various peptides solubilized in DM micelles, methanol and buffer. The peptides were 5–7.5 μM in 10 mM potassium phosphate buffer (pH 7.5) plus 4 mM DM (*solid triangles*), or 10 μM in methanol (*solid diamonds*) or in buffer alone (*open circles*). The fluorescence emission spectra were recorded with $\lambda_{ex} = 280$ nm and slit widths of 1.25 mm at both excitation and emission. They were corrected for blank spectra. The λ_{max} values plotted are the average over duplicate measurements. The temperature was 20 °C

experiments, P13) to three lifetime populations detected (Table 1). One major long lifetime population (3–4.7 ns for the various peptides) dominates the decay with a normalized amplitude of ~70–80%. Two minor populations are also present in the nanosecond (1–2 ns) and sub-nanosecond time range, both with a normalized amplitude of 5–20%. The variation of the mean lifetime $<\tau>$ with the Trp position in the peptides (Fig. 3) clearly shows that they can be divided into two groups: the first one including peptides P3, P5 and P7 and characterized by a mean lifetime of ~2.5 ns, and a second one including P9, P11 and P13 with a mean lifetime of ~4 ns. This variation is mainly due to the increase in the longest lifetime values. These changes do not arise owing to different interactions with the isotropic solvent, which was the same in all cases. This suggests an effect of the peptide local structure and/or dynamics on the Trp fluorescence intensity decays parameters and/or an effect of the neighboring residues. The Trp in P3 is close to two lysine residues situated at positions 1 and 2, which may efficiently quench its fluorescence emission by proton transfer (Chen and Barkley 1998). Moreover, Lys2 and Cys3, situated about one helical turn further from Trp5 and Trp7, respectively, may also quench their fluorescence either by proton (Lys) or electron transfer (Cys) (Chen and Barkley 1998).

In DM, with the emission wavelength set at the maximum of emission for each peptide, the Trp fluorescence intensity decays were even more complex than in methanol. Three major lifetimes were detected, with in some cases an additional minor short one that represents at most 1% of the intensity (Table 1). The longer lifetime value (5.4–4.7 ns) was significantly higher than or similar to that in methanol and, as before, this long lifetime dominates the fluorescence decay, as seen from the partial intensity values. However, in contrast to the behavior in the organic solvent, its amplitude drastically decreased from P3 to P13 (61% to 22%), but its value only decreased slightly (Table 1). As a consequence, the mean lifetime decreases with the Trp position by a factor of two from P3 to P13, in a strikingly different manner from that observed in methanol. As for variation in λ_{max}, this decrease also appears to be correlated with the Trp location within the micelle and the quenching effects by the Lys and Cys residues suggested above are no more apparent. Here, the factors influencing the decay parameters are more likely to be the local peptide conformation and local order. The micellar medium is expected to stabilize the α-helical conformation of the peptides and to reduce the Trp and helix motions.

Trp rotational dynamics: time-resolved fluorescence anisotropy decays of the model peptides in methanol and in DM micelles

In methanol, analysis of the polarized fluorescence decays by a one-dimensional model of the anisotropy

Table 1 Parameters of the intensity decays of the peptides in methanol or DM micelles. MEM analysis was performed on the fluorescence intensity $I(t)$ reconstructed from the parallel and perpendicular polarized components $I_{vv}(t)$ and $I_{vh}(t)$, such as: $I(t) = I_{vv}(t) + 2\beta_{corr}I_{vh}(t) = \Sigma\alpha_i \exp(-t/\tau_i)$, where τ is the excited state lifetime, α is its amplitude and β_{corr} is the correction factor accounting for the difference in transmission of the $I_{vv}(t)$ and $I_{vh}(t)$ components[a]

Peptide	Solvent	τ_1 (ns) α_1 I_1[c]	τ_2 (ns) α_2 I_2	τ_3 (ns) α_3 I_3	τ_4 (ns) α_4 I_4	$<\tau>$[b]
P3	MeOH	–	0.82	3.06	–	2.80
		–	0.12	0.87	–	
		–	0.03	0.97	–	
P5		0.24	0.76	3.07	–	2.42
		0.07	0.19	0.73	–	
		0.01	0.06	0.93	–	
P7		0.09	0.96	3.29	–	2.45
		0.17	0.13	0.70	–	
		0.01	0.05	0.94	–	
P9		0.49	1.98	4.72	–	4.10
		0.09	0.09	0.82	–	
		0.01	0.04	0.95	–	
P11		0.49	2.10	4.48	–	4.02
		0.05	0.12	0.83	–	
		0.01	0.06	0.93	–	
P13		0.17	1.16	4.72	–	3.94
		0.11	0.07	0.81	–	
		0.01	0.02	0.97	–	
P3	DM	–	0.60	2.80	5.42	4.08
		–	0.15	0.24	0.61	
		–	0.02	0.17	0.81	
P5		0.31	0.73	2.37	5.14	2.90
		0.09	0.19	0.35	0.37	
		0.01	0.04	0.29	0.66	
P7		0.21	0.83	2.49	4.95	2.43
		0.14	0.24	0.37	0.26	
		0.01	0.08	0.38	0.53	
P9		0.14	0.58	2.18	4.91	2.78
		0.01	0.25	0.37	0.37	
		$\ll$0.01	0.05	0.29	0.65	
P11		–	0.64	2.21	4.82	2.08
		–	0.41	0.38	0.20	
		–	0.14	0.40	0.46	
P13		–	0.51	2.04	4.70	2.11
		–	0.33	0.45	0.22	
		–	0.07	0.44	0.49	

[a]Peptides were 10 μM in methanol or in 10 mM potassium phosphate buffer, pH 7.5, containing 4 mM DM, at 20 °C. In methanol, λ_{em} was 338 nm. In DM solution, λ_{em} was set at the emission maximum of each peptide. λ_{ex} was always 280 nm. The parameters given are the normalized area (α_i) and the barycenter (τ_i) of the lifetime distribution obtained by the maximum entropy method
[b]The mean lifetime $<\tau>$ was calculated as $<t> = \Sigma\alpha_i\tau_i$
[c]The partial intensity of the lifetime τ_i was calculated as $I_i = \alpha_i\tau_i / <\tau>$. Results in methanol are representative of two series of experiments. Resulting errors on $<\tau>$ are of the order of ± 0.05

(where each lifetime is a priori associated with all modes of rotation) revealed two rotational correlation times for all peptides (Table 2). The longest one (θ_2) of ~1.3 ns probably describes the overall Brownian rotational motion of the whole peptide in the solvent, whereas the sub-nanosecond component (θ_1) (0.1–0.3 ns) should mainly describe the local rotational motion of the indole ring around the C_α-C_β-C_γ bonds. The initial anisotropy value ($A_{t=0} = \Sigma\beta_i$) was significantly lower than expected

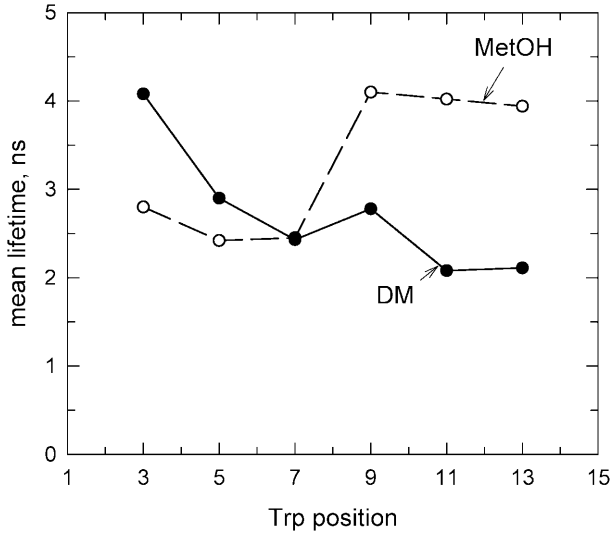

Fig. 3 Effect of Trp position on the mean lifetime, $<\tau>$, of the various peptides solubilized in methanol (*open circles*) or in DM micelles (*closed circles*). The experiments and data treatment were performed as described in Table 1

for an immobilized Trp residue (0.173; Valeur and Weber 1977), indicating that faster rotational depolarization motions are probably present but are not measurable with the time resolution of the instrumentation (~100 ps). A large semi-angle of the wobbling-in-cone sub-nanosecond rotation (ω_{max}) was calculated ($52 \pm 4°$) (Kinosita et al. 1977; see also Ichiye and Karplus 1983; Vincent and Gallay 1991), independent of the position of Trp in the peptide.

Two rotational correlation times were also observed for the peptide incorporated in DM micelles (Table 2). Each was at least one order of magnitude greater than the corresponding one in methanol. The longest one (θ_2) (mean value of 36 ns) was of the order of magnitude expected for the rotation of a spherical particle of the size of the DM micelle, according to the Perrin-Einstein expression ($\theta = V_h\eta/RT$, where V_h is the hydrated volume of the particle, η is the solvent viscosity, R the molar gas constant and T the absolute temperature) (de Foresta et al. 1999). Therefore, it probably partly reflects the Brownian rotation of the entire micelle-peptide complex. What can be related to the local motion (see θ_1) occurred in the nanosecond time scale (~3 ns). No regular variation of θ_1 with the position of the Trp residue was evidenced, whereas its proportion (β_1) increased with the penetration of the Trp residue within the micelle (Table 2). As in methanol, sub-nanosecond rotational motions faster than the limit of detection of our instrument were also present. However, the mean value of the calculated semi-angle of the wobbling-in-cone sub-nanosecond motion (30°) was much smaller than in methanol, highlighting the rotational constraints imposed by the micelle on the rotational degree of freedom of the indole ring. Similar rotational constraints were observed for TOE in DM micelles (de Foresta et al. 1999).

Table 2 Parameters of the fluorescence anisotropy decays of the peptides in methanol and in DM micelles. The fluorescence anisotropy is assumed to be described by a sum of exponentials: $A(t) = \frac{I_{vv}(t) - \beta_{corr} I_{vh}(t)}{I_{vv}(t) + 2\beta_{corr} I_{vh}(t)} = \sum_i \beta_i \exp(-t/\theta_i)$, where $I_{vv}(t)$ and $I_{vh}(t)$ are the parallel and perpendicular polarized fluorescence decays, respectively, and β_{corr} is a factor correcting for the difference of transmission by the emission monochromator of $I_{vv}(t)$ and $I_{vh}(t)$

Peptide	Medium	θ_1 (ns) β_1	θ_2 (ns) β_2	ω_{max} (°)[a]	A_s[b]
P3	MeOH	0.15 ± 0.05 0.064 ± 0.033	1.4 ± 0.03 0.052 ± 0.006	49 ± 2	0.024
P5		0.35 0.023	1.1 0.047	50	0.021
P7		0.30 0.059	1.8 0.032	57	0.023
P9		0.10 0.018	0.9 0.047	50	0.013
P11		0.34 0.052	1.4 0.034	56	0.016
P13		0.13 0.094	1.0 0.051	49	0.019
P3	DM micelles	2.6 0.015	27 0.108	28	0.098
P5		4.1 0.020	33 0.101	28	0.100
P7		2.1 0.023	40 0.093	29	0.104
P9		3.5 0.021	34 0.072	36	0.086
P11		2.5 0.032	39 0.066	34	0.094
P13		2.4 0.030	43 0.088	29	0.105

[a]The semi-angle ω_{max} of the wobbling-in-cone sub-nanosecond motion was calculated in methanol from: $\frac{\beta_2}{A_0} = [1/2 \cos w_{max} (1 + \cos w_{max})]^2$ and in DM micelles as: $\frac{\sum_i \beta_i}{A_0} = [1/2 \cos w_{max} (1 + \cos w_{max})]^2$, where A_0 is the anisotropy in the absence of depolarization. At an excitation wavelength of 280 nm, it displayed a value of 0.173, which was used for the calculations (Valeur and Weber 1977)

[b]Steady-state anisotropy. Experimental conditions as in Table 1

Although the one-dimensional analysis appears satisfactory in terms of statistic criteria (χ^2), a two-dimensional (τ versus θ) analysis was also carried out in which no a priori association exists between lifetime and rotational correlation time (Brochon 1994; Vincent et al. 2000b). No peculiar τ versus θ associations were observed (data not shown).

Trp fluorescence quenching of the model peptides in mixed micelles of DM with brominated derivatives

Figure 4 illustrates the Trp steady-state fluorescence quenching experiments of the peptides with the brominated detergents. This figure shows the quenching curves of P13 in mixed micelles of DM with either BrDM or BrUM. We fitted the quenching model already described for quenching in membranous systems (London and Feigenson 1981; East and Lee 1982) to the data. The validity of this model has already been analyzed in

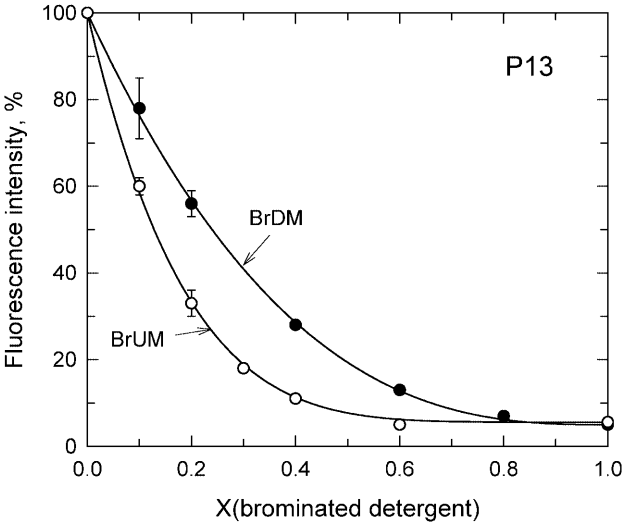

Fig. 4 Quenching of P13 fluorescence in mixed micelles of BrDM/DM (*closed circles*) or BrUM/DM (*open circles*). P13 (5 μM) was added to 10 mM potassium phosphate buffer (pH 7.5) containing, in addition, a mixture of BrDM and DM, or BrUM and DM, at a final total detergent concentration of 4 mM, at 20 °C. The resulting fluorescence intensity was recorded for 150 s to allow equilibration and the final fluorescence intensity was corrected for blank value (detergents in buffer) and plotted as a function of the molar fraction of brominated detergent X, defined as $X = (\text{BrDM})/[(\text{BrDM}) + (\text{DM})]$ or $(\text{BrUM})/(\text{BrUM}) + (\text{DM})]$. X was varied between 0 (pure DM micelles) and 1 (pure BrDM or BrUM micelles). λ_{ex} was set at 280 nm and λ_{em} at 312 nm, with slit widths of 1.25 mm at both excitation and emission. Data points are the mean of duplicate measurements. The function $F/F_0 = (1 - F_{min}/F_0)(1 - X)^n + F_{min}/F_0$ was fitted to the data (see Materials and methods)

micellar systems (de Foresta et al. 1999) (see Materials and methods for details). For P13, the same residual fluorescence ($F_{min}/F_0 = 6\%$) was obtained in both pure brominated detergent micelles (i.e. for $X = 1$). Otherwise, the curves differ for $0 < X < 1$, the n parameter reflecting the accessibility of Trp to the bromine atoms located in the detergent acyl chains, being 2.7 and 5.5 in BrDM and BrUM, respectively. P13 is the peptide for which the difference between these two values was the greatest.

Figure 5 summarizes the results obtained for all peptides. Panel A shows the variations in the residual fluorescence F_{min}/F_0 (at $X = 1$). In all cases, this residual fluorescence was quite low, below 15%, with slight variations from 2 to 13% which may be correlated with the n values (see below). In addition, the curve of F_{min}/F_0 in BrDM was lower than that in BrUM. These data indicate that, regardless of the position of Trp in these various peptides, only a small fraction of Trp is, on average, out of reach of the detergent alkyl chain bromines in these conditions. Panel B shows the variations in the parameter n, reflecting the accessibility of Trp to the brominated chains, as a function of the Trp position in the peptide. All n values were higher in BrUM than in BrDM. In addition, in BrUM (upper curve) there was a steady increase in n from P5 to P13, which strongly suggests that this variation directly reflects Trp depth in

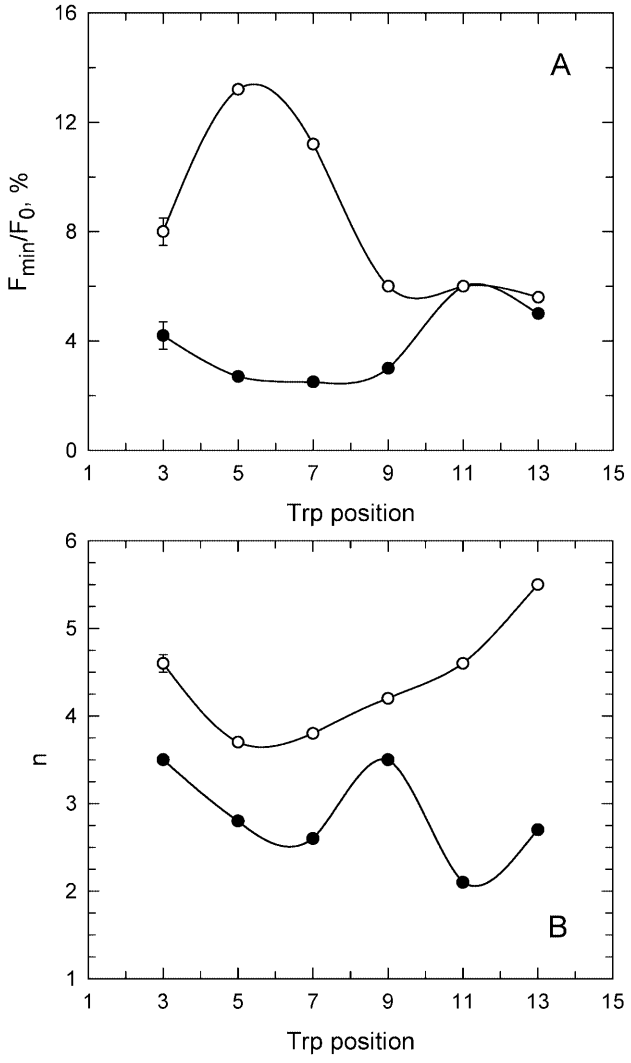

Fig. 5 Variations of the parameters F_{min}/F_0 (**A**) and n (**B**) of the peptide quenching curves in mixed detergent micelles, as a function of Trp position. The quenching curves of the six model peptides (P3 to P13) in mixed micelles of BrDM/DM (*closed symbols*) or BrUM/DM (*open symbols*) were constructed as described in the legend to Fig. 4. λ_{em} was set at the emission maximum wavelength of each peptide (i.e. 327–313 nm for P3 to P13). All the fits were performed as for P13

the micelles: when n is highest, Trp is closest to the center of the micelle. This seems logical, because BrUM is brominated at the end of the alkyl chain and even if the chains are more or less disordered (see discussion below), the distribution probability of bromine is expected to be higher in the center of the micelle. P3 behaved in an unusual manner: this may be due to a peculiar folding of some of the alkyl chains which, instead of being extended, fold back so that their extremity could come close to the polar head region. At first sight, the curve obtained with BrDM (Fig. 5B, lower curve) is more complicated. However, the same reasoning as above seems to apply. In this case, the bromines are at intermediary positions on the alkyl chains (C7 and C8) and their most probable positions are no longer in the center of the micelle but at intermediary positions between the center and the polar heads, close to W9 (in P9). All the other Trps locations are more remote from the bromines in the micelle and are characterized by lower n values, except for P3; if a chain folding hypothesis is again suggested, a preferred conformation of the chain should be one bringing the bromines on C7 and C8 to the level of the polar headgroup. However, although this curve seems logical, it seems difficult from quenching with BrDM alone to derive the Trp depth unequivocally because the same n values were obtained for different Trp positions.

The mechanism of quenching by the bromine atoms in mixed micelles of DM with BrUM was also studied by fluorescence intensity decay measurements on two of the six peptides, P3 and P9. The molar fraction of BrUM was only varied between 0 and 0.4, so that the residual fluorescence intensity of the peptides was not too low. This experiment aimed to delineate the contributions of static and dynamic quenching to the overall quenching.

The parameters of the intensity decays are shown in Table 3. For P3, the values of the three lifetimes decreased. This indicates a dynamic quenching process. However, this decrease was lower than that of the overall fluorescence (shown in Fig. 6), which also indicates a contribution from a static quenching mechanism. In addition, a change in the lifetime distribution occurred, the relative amplitude of the longest lifetime being reduced in favor of that of the shorter one. This may indicate that there are less steric hindrances for the quenching of the rotamer with the longest lifetime than for the others. It is likely that the dynamic contribution occurs owing to the alkyl chain motions during Trp lifetime rather than to an overall exchange of non-brominated with brominated detergent in the local environment of the peptide, which probably occurs more slowly than the nanosecond time scale. The static contribution is due to quenching by brominated chains with bromines already close to Trp at the time of excitation. Figure 6 shows the variations in the mean lifetime of P3 compared to its steady-state intensity variations. The two curves seem to move apart significantly for BrUM molar fractions higher than 0.2. At a low BrUM molar fraction (< 0.2), dynamic quenching should be preponderant, whereas above $X = 0.2$, static quenching should begin to be significant. Very similar trends were observed for P9 quenching in mixed micelles of DM with BrUM (Table 2 and Fig. 6). These data, that we believe are mainly dependent on alkyl chain motions, are probably representative of what occurs with the other peptides and with BrDM.

CD spectra of the model peptides in DM micelles and in methanol

The secondary structure of the model peptides was assessed from the CD spectra in DM micelles and in methanol. In methanol (Fig. 7A), all the spectra (except for P7, see below) are very similar and exhibit an overall

Table 3 Parameters of the intensity decays of P3 and P9 in mixed micelles of DM/BrUM[a]

Peptide	*X*(BrUM)	α_1	α_2	α_3	τ_1 (ns)	τ_2	τ_3	$<\tau>$
P3	0	0.15	0.24	0.61	0.59	2.80	5.42	4.08
	0.1	0.23	0.26	0.51	0.52	2.67	4.82	3.16
	0.2	0.30	0.24	0.46	0.17	1.04	3.82	2.05
	0.3	0.32	0.22	0.46	0.14	0.72	3.08	1.63
	0.4	0.48	0.29	0.23	0.15	1.16	3.50	1.21
P9	0	0.25	0.36	0.37	0.58	2.18	4.91	2.78
	0.1	0.25	0.41	0.34	0.34	1.26	3.53	1.86
	0.2	0.42	0.31	0.28	0.11	0.82	2.75	1.06
	0.3	0.38	0.31	0.32	0.11	0.61	2.24	0.94
	0.4	0.54	0.30	0.15	0.13	0.70	2.21	0.67

[a]Peptides were 10 μM in 10 mM potassium phosphate buffer, pH 7.5, containing 4 mM total detergent concentration [(DM) + (BrUM)], at 20 °C. The molar fraction of BrUM, *X*(BrUM), was varied as indicated. λ_{ex} was set at 280 nm. λ_{em} was set at 327 nm and 321 nm for P3 and P7, respectively. The parameters of the decays are as defined in Table 1

shape characteristic of an α-helix CD signal: a positive peak was observed below 200 nm (at 192 nm) and two negative minima above 200 nm (a major one at 208 nm and a plateau in the 216–222 nm region). Relative peak heights $\theta_{192}/\theta_{208}/\theta_{222}$ (relative to θ_{222} taken as 1) were in the ratio 2.8/1.4/1. The absolute ellipticity of P7 was slightly lower throughout the spectrum and the positive peak was slightly red-shifted (up to 194 nm) and of relative lower height (2.1 instead of 2.8). Estimation of the α-helical content of the peptides from the ellipticity value at 222 nm, taking into account the helix length (see Materials and methods), yielded a mean value of $76 \pm 2\%$ for all peptides except P7 (67%).

For the peptides embedded in DM micelles, the overall shape of the spectra resembles that obtained in methanol, with only small differences. First, there was a slight dispersion effect of this anisotropic medium on peptide structure, because the various spectra do not superimpose as well as in methanol (Fig. 7B). Second, the positive peak was located at 192–193 nm and the negative minima at 208 nm and 218–222 nm. The shape of the spectra was also slightly distorted with respect to those in methanol, with closer amplitudes of the two minima at 208 and 222 nm in DM (relative height ratios defined as above are, as a mean for all peptides except P7, 2.9/1.2/1, and for P7, 2.8/0.9/1). Note that the mean $\theta_{208}/\theta_{222}$ ratio of 1.2 is similar to that expected for monomeric peptides (1.25), whereas this value is lowered to 1 in dimeric coiled-coil structures (Goetz et al. 2001 and references therein). Here again, the peptides were also mainly in an α-helical structure but with a slightly lower helical content for P3, P5 and P7 (62%, 66% and 57%, respectively) than for P9, P11 and P13 (77%, 73% and 80%, respectively).

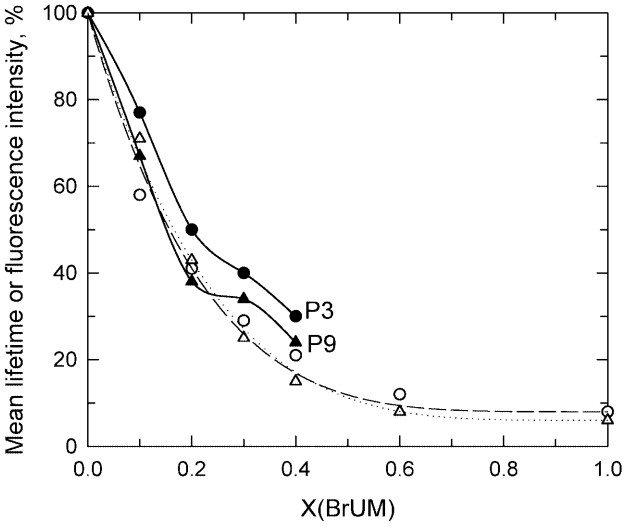

Fig. 6 Relative variations of the mean lifetime of P3 (*closed circles*) and P9 (*closed triangles*) with the molar fraction of BrUM in mixed BrUM/DM micelles. The data were obtained as explained in the legend to Table 1. The data were compared to the relative steady-state intensity of P3 (*open circles*, *dashed line*) and P9 (*open triangles*, *dotted line*) obtained as described in the legend to Fig. 4

Discussion

This paper clearly shows a position-dependent variation of various spectroscopic parameters of Trp-containing model peptides inserted into detergent micelles and precisely quantifies these parameters.

We chose experimental conditions (a large excess of detergent molecules over peptides) under which the peptides were fully solubilized by detergent micelles. This was shown by Trp fluorescence emission spectra characteristic of hydrophobic environments and by the stability of the fluorescence intensity. The CD signal was also stable over time. The excess of detergent was also chosen to favor the formation of peptide-detergent complexes with a single peptide per complex. The formation of peptide multimers was shown to be concentration dependent for hydrophobic peptides inserted in lipid membranes. Here, in addition to the excess of detergent molecules, the segregation of peptides in separated micelles (in contrast to the continuous membrane phase in vesicles bilayers) is an additional factor for avoiding peptide aggregation.

The model peptides insert radially within DM micelles

The measured fluorescence parameters imply that the peptides (assimilated to helix rods, see below) were

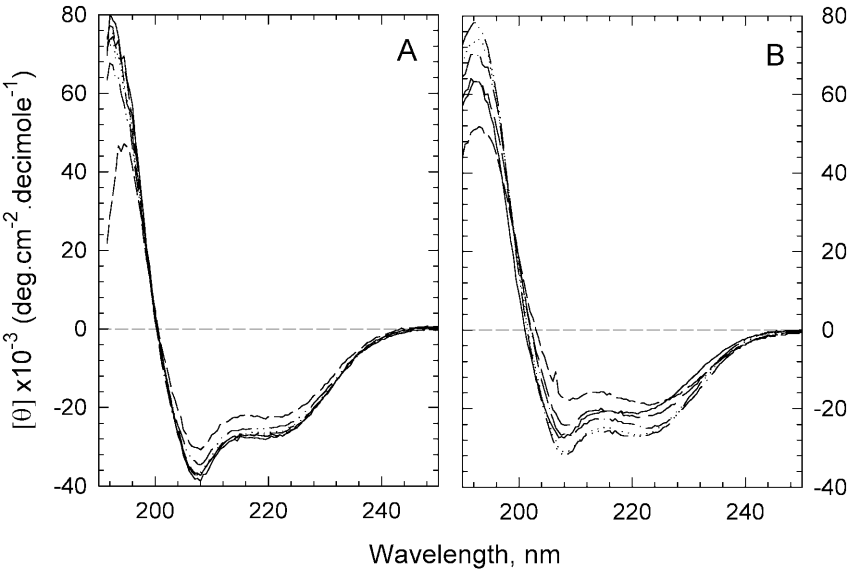

Fig. 7 CD spectra of the six model peptides solubilized in methanol (**A**) or in DM micelles (**B**). **A** Peptides were 25 μM in methanol: P3 (*solid line*), P5 (*medium dash*), P7 (*short dash*), P9 (*dot*), P11 (*dash-dot*), P13 (*dash-dot-dot*). **B** Peptides were 25 μM in 10 mM potassium phosphate buffer containing 4 mM DM; symbols are as in **A**

inserted into the DM micelles so that their long axes were orientated radially within the micelles. This is shown both by the steady variations and values of λ_{max} corresponding to a polarity gradient through the micelle interior. Variations in λ_{max} values were also observed for amphiphilic peptides inserted in parallel into a detergent or lipid membrane surface with Trp either on the polar or apolar face of the peptide. However, in this case, λ_{max} values should be red-shifted, to around 330–340 nm, corresponding to an intermediate and highly polar environment (Mangavel et al. 1998; Clayton and Sawyer 1999). A cyclic λ_{max} variation should also be obtained, depending on the position of the Trp residue along the peptide sequence. The radial insertion of the polyLeu peptides is further supported by the high peptide quenching efficiencies observed with both brominated detergents used, the bromine atoms of which were either close to the middle (for BrDM) or at the end (for BrUM) of the detergent alkyl chain.

As in lipid bilayers, a polarity gradient is detected within DM micelles

Thus, the hydrophobic core of the micelle (or more precisely, the peptide-detergent complex) cannot be assimilated to a bulk apolar phase. The very low λ_{max} values for the deeper Trp (in P13) are in agreement with results from molecular dynamics simulation studies on two detergents with similar alkyl chains (C12): sodium dodecyl sulfate (SDS) and dodecylphosphocholine (DPC) (MacKerell 1995; Tieleman et al. 2000). For SDS, no water molecules entered the interior of the micelles during the simulation period (120 ps). This is also true for DPC micelles, with simulations of up to 15 ns. In micelles with well-defined hydrophobic cores, we recently showed that the polar headgroup of DM is less permeant to water-soluble quenchers than either DPC or another C12 chain detergent, $C_{12}E_8$ (Tortech et al. 2001). For comparison with lipid bilayers, the same peptides, embedded in C18:1PC lipid vesicles in which they adopt a transmembrane orientation, exhibit a λ_{max} dependence from 314 to 338 nm (Ren et al. 1997); therefore, a similar low polarity (due to the absence of water) is observed in the center of the lipid bilayer and of the detergent micelle, but, close to the headgroup region, the polarity sensed by the peptide Trp (e.g. in P3) is significantly lower in DM micelles than in C18:1PC vesicles. With a similar peptide with a central Trp (Ac-$K_2GL_7WL_9K_2A$-amide) embedded in C18:1PC, the polarity of the bilayer center was also reported to be very low, because its λ_{max} exhibited a ~20 nm blue-shift compared to the λ_{max} obtained in methanol (323 and > 340 nm in bilayer and methanol, respectively) (Webb et al. 1998). Other Trp-flanked hydrophobic model peptides exhibit fluorescence maxima around 337 nm in various lipid bilayers (De Planque et al. 2001), whereas other hydrophobic peptides containing a single, nearly central, Trp such as slightly modified polyAla peptides (Liu and Deber 1997) have also been studied in lipid micelles (lysoPC and lysoPG) or vesicles but, in this case, the peptide was shown to be of mixed orientation (parallel and perpendicular to the surface) and the λ_{max} values corresponded to intermediate polarity.

Depth-dependent quenching of the peptides Trp is observed with each brominated detergent, BrDM and BrUM

The steady-state quenching experiments on peptide Trp with both brominated detergents confirmed the location of all peptide Trps within the detergent micelle, due in particular to the high quenching observed in the high brominated detergent molar fraction. The quenching

curve analysis indicates that the two parameters n and F_{min}/F_0 (see Results) exhibit a Trp position-dependent pattern specific for each brominated detergent. Keeping in mind that Trp quenching results from Trp-bromine(s) contacts, such patterns can be explained by a relative disorder of the alkyl chain making different positions available for bromine atoms (with different probabilities). In particular, the P3 quenching results suggest that the alkyl chain sometimes folds such that the bromine atoms come close to the polar headgroups. When compared to the quenching results previously obtained with TOE as a model compound, we note that n was equal to 3.7 for TOE quenching curves with BrDM, i.e. close to the value obtained here for P3 (and also for P9, but the λ_{max} of P9 and TOE are quite different). In addition, n (for TOE) was 3.6 with BrUM, i.e. close to the value obtained here for P5. This is consistent with our previous proposed location for TOE, i.e. inside the micelles and close to the headgroup region. We also noted that the insertion of Trp within a peptide did not significantly lower its accessibility to the alkyl chains when compared to the smaller compound, TOE.

Different position-dependent lifetime distributions are characterized in methanol and in DM micelles

Time-resolved fluorescence decays of the various peptides were heterogeneous both in methanol and in DM and showed a different Trp position-dependent variation in these two media. What does this tell us about peptide intrinsic properties and the environment? The generally accepted interpretation of Trp lifetime heterogeneity in proteins and peptides is the presence of different rotamers around the C_α-C_β bond (Szabo and Rayner 1980; Willis et al. 1994). Relative populations and the exchange rate between these rotamers may vary along the peptide; this should be reflected by the lifetime values and their amplitudes. The effect of the chemical environment and of dipolar relaxation phenomena is also to be considered (e.g. Vincent et al. 1995, 2000a; Ladokhin and White 2001). In methanol, an isotropic solvent which does not induce any particular position-dependent behavior, the value of the longest lifetime that dominates the decay was constant from P3 to P7 and increased suddenly from position P7 to P9 and then remained constant. This sharp Trp position dependence of the major lifetime is thought to be due to the intrinsic characteristics of the peptide: local dynamics and/or a particular sequence. Fluorescence anisotropy decay measurements, performed to monitor the local Trp dynamics, did not show any significant differences in the semi-angle ω_{max} characterizing the sub-nanosecond rotational motions of the Trp residue in the peptides dissolved in methanol as a function of its position along the sequence. As for the sequence, the local amino acid sequences including the Trp residues are different for the first three peptides as compared to the others. Thus, in P3 (sequence K-K-W-L-) and P5 (K-K-C-L-W-L-) the Trp long lifetime may be respectively reduced by quenching by Lys1 and Lys2, respectively, by proton exchange (Chen and Barkley 1998), while in P7 (K-K-C-L-L-L-W-L-) the Cys3 residue may act as an efficient quencher. In contrast, the amplitude of this long lifetime remained constant at high values along the peptide chain in methanol. This lifetime population may correspond to the major t rotamer that is favored in α-helical sequences (Penel et al. 1999), as previously suggested (Willis et al. 1994; Bouhss et al. 1996).

The opposite variation of the mean lifetime with Trp position was observed when the peptides were embedded in DM micelles (decreasing from P3 to P13) as compared to methanol. This effect is the result of a decrease in the long lifetime amplitude, the lifetime values staying almost constant. In these conditions, some of the peptides have a lower α-helical content than in methanol. This may explain the differences in rotamer distributions. In addition, the anisotropic medium of the micelle may have an effect. These results are also strengthened by the observation of a similar decrease in the mean lifetime of the same peptides embedded in the zwitterionic detergent DPC (de Foresta B, Vincent M, Gallay J, unpublished results).

Fluorescence anisotropy probably reflects both hindered local motion of the peptides and whole micelle rotation

Fluorescence anisotropy decay measurements are expected to provide information on local Trp motion, segmental motions of the peptide and whole peptide rotation, as well as the rotation of the peptide-detergent complex in DM. All these motions occur on the sub-nanosecond and nanosecond time range. In addition, if asymmetric rotors are involved, the resulting anisotropy decay should imply many exponential terms (Ichiye and Karplus 1983). However, if the various rotational correlation times are close to one another, they will not be resolved in the experimental decay. In methanol, two components of the anisotropy decay are obtained, with a difference in their values of about one order of magnitude (0.1–0.3 ns and ~1 ns). They are consistent with previous measurements in methanol, with slightly shorter helical peptides (21 amino acids long), analogs of alamethicin, for which rotational correlation times of 0.1–0.2 ns and ~0.6 ns were obtained (Vogel et al. 1988). In DM micelles, two components of the decay are also evidenced but shifted to the nanosecond range. The first three motions are slowed in DM as compared to methanol, owing to the constraints imposed by the micelle. These constraints can be assigned to the strong packing forces between the bulky maltoside moieties (forming the water/micelle interface) that govern the self-assembly of the monomers to form the micelles (Dupuy et al. 1997). However, there is not a clear dependence of Trp motional properties with Trp depth. Similar constraints on the rotational motion of Trp were

also described for hydrophobic (and/or amphiphilic) peptides inserted in lipid vesicles either in a transverse position or parallel to the membrane surface (Vogel et al. 1988; Clayton and Sawyer 2000; Talbot et al. 2001). Here, the longer component of the decay also probably reflects the whole micelle rotation.

Quenching of the peptides by brominated detergents involves both static and dynamic contributions

The time-resolved quenching experiments performed with P3 and P9 as examples and with BrUM as the brominated detergent yielded a complex pattern. Both static and dynamic quenching were observed and their relative contribution depended upon the brominated detergent molar fraction in the micelle. The contribution of dynamic quenching was higher than previously observed with TOE and the rationale for this might be the presence of a longer lifetime component (with a higher amplitude) in peptides than in TOE [$\tau_3 = 5.4$ and 4.9 ns for P3 and P9, respectively, compared to $\tau_4 = 4.3$ ns for TOE (de Foresta et al. 1999); see Fig. 4]. There is, therefore, slightly more time for the bromines (on the alkyl chains) to diffuse towards the Trp during its excited-state lifetime.

Peptide secondary structure and model of peptide-detergent complex

Our CD experiments showed that the model fluorescent peptides adopted a predominantly α-helical structure in methanol at 20 °C. The mean α-helix content obtained, 76%, corresponds to 19 of the 25 residues and probably corresponds to the whole hydrophobic region of the peptide, excluding the K_2C and K_2A N- and C-terminal ends. This is consistent with previous findings in poly-Leu-type peptides in the same solvent by both CD (Davis et al. 1983) and FTIR experiments (Zhang et al. 1992a, 1992b). The remaining non α-helical structure was suggested to be an extended conformation. Therefore, at least in methanol, the insertion of Trp does not significantly perturb the structure of such peptides. In DM micelles, similar results were obtained for P9 to P13 whereas P3 and P5 were shown to have slightly lower α-helical contents. This may be due to the difficulty of accommodating the bulky Trp close to the polar DM headgroups, resulting in the destabilization of the helical structure.

As the length of α-helices increases by 1.5 Å per amino acid residue, the difference in translation (along the helix axis) between two Trp in Pi and P$i+2$ peptides embedded in DM micelles should be 3 Å (and maybe slightly more between P3 and P5), taking into account these CD results.

We can speculate about the way the peptides are inserted into the peptide-detergent complexes, taking into account the model proposed for the DM micelles (Dupuy et al. 1997). This model, fitting small-angle neutron and X-ray scattering data, describes a DM micelle as an oblate ellipsoid micelle (external diameters: 41 and 69 Å) constituted of a polar layer of constant thickness (6 Å) surrounding an ellipsoid core (diameters: 28 and 56 Å). The length of the whole peptide as (100%) α-helix would be of 36 Å and is therefore expected to insert in the micelle along the ellipsoid short axis so that the terminal polar residues are located in the polar region of the micelle (see Scheme 1). It is noteworthy that the peptide-detergent complex may not be merely the addition of one peptide to a micelle. Examples have been given in which the number of detergents in a peptide-detergent complex (with DPC as the detergent) was either slightly lower (Lauterwein et al. 1979) or higher

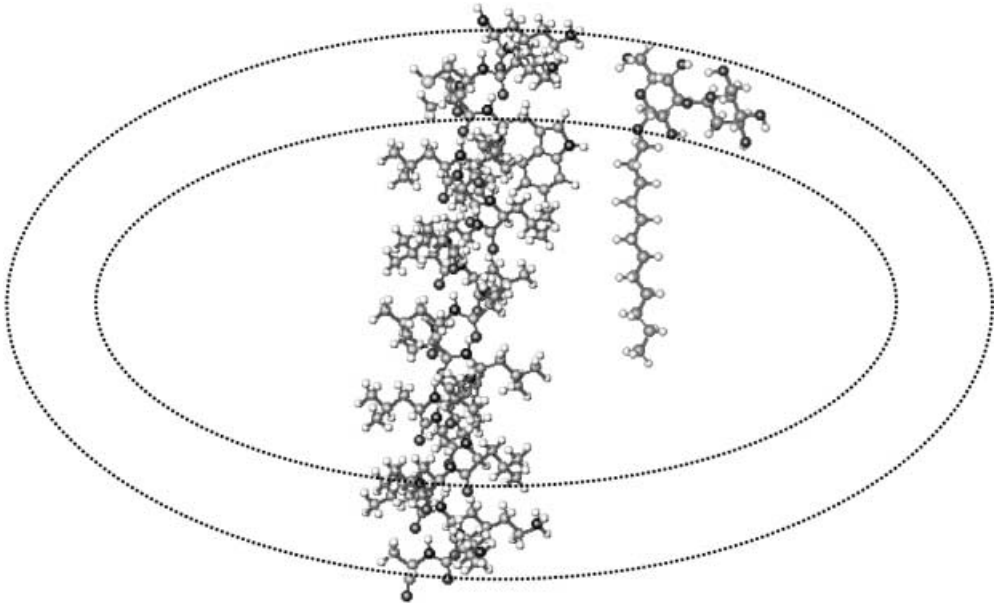

Scheme 1 Schematic representation of P5 inserted in a DM micelle. Cross-section of the micelle, with indication of the polar headgroup region (between the two *dotted ellipses*). One DM molecule is shown (with its alkyl chain in an extended conformation). P5 is represented in an α-helix conformation

(Beswick et al. 1998) than that of the pure micelle. DPC micelles, however, are much smaller than DM micelles and may be more sensitive to perturbation upon interaction with amphiphilic peptides.

Conclusions

Our results with six Trp-containing hydrophobic model peptides provide evidence for the formation of peptide-detergent (DM) complexes in which Trp senses different environments according to its different depths within the complexes (see Scheme 1). The Trp, located at intervals of ~3 Å (along the peptides), exhibits significant variations in λ_{max}, and in lifetime distributions. Trp rotational correlation time distributions reflect both the rotation of the whole complex and the local motion of Trp, which is much slower than in methanol. Peptide Trps show a characteristic pattern of quenching by two brominated analogs of DM. In addition to giving more detailed insight into the characteristics of detergent micelles, extending previous model systems studies (de Foresta et al. 1999; Tortech et al. 2001), these data provide useful references for the analysis of fluorescent amphipathic (or hydrophobic) peptide insertion in such membrane-mimetic systems.

Acknowledgements We thank the technical staff of the Laboratoire pour l'Utilisation du Rayonnement Electromagnétique (LURE) for running the synchrotron ring during the beam sessions. We thank Dr. A. Sanson and J.-B. Arlot for help in the CD experiments.

References

Belohorcová K, Davis JH, Woolf TB, Roux B (1997) Structure and dynamics of an amphiphilic peptide in a lipid bilayer: a molecular dynamics study. Biophys J 73:3039–3055

Beswick V, Guerois R, Cordier-Ochsenbein F, Coïc Y-M, Huynh-Dinh T, Tostain J, Noël J-P, Sanson A, Neumann J-M (1998) Dodecylphosphocholine micelles as a membrane-like environment: new results from NMR relaxation and paramagnetic relaxation enhancement analysis. Eur Biophys J 28:48–58

Bouhss A, Vincent M, Munier H, Gilles A-M, Takahashi M, Bârzu O, Danchin A, Gallay J (1996) Conformational transitions within the calmodulin-binding site of *Bordetella pertussis* adenylate cyclase studied by time-resolved fluorescence of Trp242 and circular dichroism. Eur J Biochem 237:619–628

Brochon JC (1994) Maximum entropy method of data analysis in time-resolved spectroscopy. Methods Enzymol 240:262–311

Chen Y, Barkley MD (1998) Toward understanding tryptophan fluorescence in proteins. Biochemistry 37:9976–9982

Chen Y-H, Yang JT, Chau KH (1974) Determination of the helix and β form of proteins in aqueous solution by circular dichroism. Biochemistry 13:3350–3359

Clayton AHA, Sawyer WH (1999) Tryptophan rotamer distributions in amphipathic peptides at a lipid surface. Biophys J 76:3235–3242

Clayton AHA, Sawyer WH (2000) Site-specific tryptophan dynamics in class A amphipathic helical peptides at a phospholipid bilayer interface. Biophys J 79:1066–1073

Davis JH, Clare DM, Hodges RS, Bloom M (1983) Interaction of a synthetic amphiphilic polypeptide and lipids in a bilayer structure. Biochemistry 22:5298–5305

De Planque MRR, Goormaghtigh E, Greathouse DV, Koeppe II RE, Kruijtzer JAW, Liskamp RMJ, Kruijff B de, Killian JA (2001) Sensitivity of single membrane-spanning α-helical peptides to hydrophobic mismatch with a lipid bilayer: effects on backbone structure, orientation, and extent of membrane incorporation. Biochemistry 40:5000–5010

Dupuy C, Auvray X, Petipas C, Rico-Lattes I, Lattes A (1997) Anomeric effects on the structure of micelles of alkyl maltosides in water. Langmuir 13:3965–3967

East JM, Lee AG (1982) Lipid selectivity of the calcium and magnesium ion dependent adenosinetriphosphatase, studied with fluorescence quenching by a brominated phospholipid. Biochemistry 21:4144–4151

Epand RM, Vogel HJ (1999) Diversity of antimicrobial peptides and their mechanisms of action. Biochim Biophys Acta 1462:11–28

Foresta B de, Legros N, Plusquellec D, Maire M le, Champeil P (1996) Brominated detergents as tools to study protein-detergent interactions. Eur J Biochem 241:343–354

Foresta B de, Gallay J, Sopkova J, Champeil P, Vincent M (1999) Tryptophan octyl ester in detergent micelles of dodecylmaltoside: fluorescence properties and quenching by brominated detergent analogs. Biophys J 77:3071–3084

Gao X, Wong TC (1999) The study of the conformation and interaction of two tachykinin peptides in membrane mimicking systems by NMR spectroscopy and pulsed field gradient diffusion. Biopolymers 50:555–568

Goetz M, Carlotti C, Bontems F, Dufourc EJ (2001) Evidence for an α-helix→π-bulge helicity modulation for the *neu/erB-2* membrane-spanning segment. A ^{1}H NMR and circular dichroism study. Biochemistry 40:6534–6540

Huschilt JC, Millman BM, Davis JH (1989) Orientation of α-helical peptides in a lipid bilayer. Biochim Biophys Acta 979:139–141

Ichiye T, Karplus M (1983) Fluorescence depolarization of tryptophan residues in proteins: a molecular dynamics study. Biochemistry 22:2884–2893

Katragadda M, Alderfer JL, Yeagle PL (2001) Assembly of a polytopic membrane protein structure from the solution structures of overlapping peptide fragments of bacteriorhodopsin. Biophys J 81:1029–1036

Kinosita K, Kawato S, Ikegami A (1977) A theory of fluorescence polarization decay in membranes. Biophys J 20:289–305

Ladokhin AS, White SH (2001) Alphas and taus of tryptophan fluorescence in membranes. Biophys J 81:1825–1827

Lauterwein J, Bösch C, Brown LR, Wüthrich K (1979) Physicochemical studies of the protein-lipid interactions in melittin-containing micelles. Biochim Biophys Acta 556:244–264

Lewis RNAH, Prenner EJ, Kondejewski LH, Flach CR, Mendelsohn R, Hodges RS, McElhaney RN (1999) Fourier transform infrared spectroscopic studies of the interaction of the antimicrobial peptide gramicidin S with lipid micelles and with lipid monolayer and bilayer membranes. Biochemistry 38:15193–15203

Liu L-P, Deber CM (1997) Anionic phospholipids modulate peptide insertion into membranes. Biochemistry 36:5476–5482

Livesey AK, Brochon JC (1987) Analyzing the distribution of decay constants in pulse-fluorimetry using the maximum entropy method. Biophys J 52:693–706

London E, Feigenson GW (1981) Fluorescence quenching in model membranes. 1. Characterization of quenching caused by a spin-labeled phospholipid. Biochemistry 20:1932–1938

MacKerell AD Jr (1995) Molecular dynamics simulation analysis of a sodium dodecyl sulfate micelle in aqueous solution: decreased fluidity of the micelle hydrocarbon interior. J Phys Chem 99:1846–1855

Mangavel C, Maget-Dana R, Tauc P, Brochon J-C, Sy D, Reynaud JA (1998) Structural investigations of basic amphipathic model peptides in the presence of lipid vesicles studied by circular dichroism, fluorescence, monolayer and modeling. Biochim Biophys Acta 1371:265–283

Penel S, Hughes E, Doig AG (1999) Side-chain structures in the first turn of the α-helix. J Mol Biol 287:127–143

Popot J-L, Engelman DM (1990) Membrane protein folding and oligomerization: the two-stage model. Biochemistry 29:4031–4037

Ren J, Lew S, Wang Z, London E (1997) Transmembrane orientation of hydrophobic α-helices is regulated both by the relationship of helix length to bilayer thickness and by the cholesterol concentration. Biochemistry 36:10213–10220

Rouvière N, Vincent M, Craescu CT, Gallay J (1997) Immunosuppressor binding to the immunophilin FKBP59 affects the local structural dynamics of a surface β-strand: time-resolved fluorescence study. Biochemistry 36:7339–7352

Schwyzer R (1995) In search of the "bio-active conformation" – is it induced by the target cell membrane? J Mol Recognit 8:3–8

Shepherd CM, Schaus KA, Vogel HJ, Juffer AH (2001) Molecular dynamics study of peptide-bilayer adsorption. Biophys J 80:579–596

Soulié S, Foresta B de, Møller JV, Bloomberg GB, Groves JD, Maire M le (1998) Spectroscopic studies of the interaction of Ca^{2+}-ATPase-peptides with dodecylmaltoside and its brominated analog. Eur J Biochem 257:216–227

Szabo AG, Rayner DM (1980) Fluorescence decay of Trp conformers in aqueous solution. J Am Chem Soc 102:554–563

Talbot J-C, Thiaudière E, Vincent M, Gallay J, Siffert O, Dufourcq J (2001) Dynamics and orientation of amphipathic peptides in solution and bound to membranes: a steady-state and time-resolved fluorescence study of staphylococcal δ-toxin and its synthetic analogues. Eur Biophys J 30:147–161

Tieleman DP, Spoel D van der, Berendsen HJC (2000) Molecular dynamics simulations of dodecylphosphocholine micelles at three different aggregate sizes: micellar structure and chain relaxation. J Phys Chem B 104:6380–6388

Tortech L, Jaxel C, Vincent M, Gallay J, Foresta B de (2001) The polar headgroup of the detergent governs the accessibility to water of tryptophan octyl ester in host micelles. Biochim Biophys Acta 1514:76–86

Valeur B, Weber G (1977) Resolution of the fluorescence excitation spectrum of indole into the ^1L_a and ^1L_b excitation bands. Photochem Photobiol 25:441–444

Vincent M, Gallay J (1991) The interactions of horse heart apocytochrome *c* with phospholipid vesicles and surfactants micelles: time-resolved fluorescence study of the single Trp residue (Trp59). Eur Biophys J 20:183–191

Vincent M, Gallay J, Demchenko AP (1995) Solvent relaxation around the excited state of indole: analysis of fluorescence lifetime distributions and spectral shift. J Phys Chem 99:14931–14941

Vincent M, Gilles A-M, Li de la Sierra I, Briozzo P, Bârzu O, Gallay J (2000a) Nanosecond fluorescence dynamic Stokes shift of tryptophan in a protein matrix. J Phys Chem B 104:11286–11295

Vincent M, Rouvière N, Gallay J (2000b) Wavelength-resolved fluorescence emission of proteins using the synchrotron radiation as pulsed-light source: cross-correlations between lifetimes, rotational correlation times and tryptophan heterogeneity in FKBP59 immunophilin. Cell Mol Biol 46:1113–1131

Vogel H, Nilsson, L, Rigler R, Voges K-P, Jung G (1988) Structural fluctuations of a helical polypeptide traversing a lipid bilayer. Proc Natl Acad Sci USA 85:5067–5071

Webb RJ, East JM, Sharma RP, Lee AG (1998) Hydrophobic mismatch and the incorporation of peptides into lipid bilayers: a possible mechanism for retention in the Golgi. Biochemistry 37:673–679

Willis KJ, Neugebauer W, Sikorska, M, Szabo AG (1994) Probing α-helical secondary structure at a specific site in model peptides via restriction of tryptophan side-chain rotamer conformation. Biophys J 66:1623–1630

Zhang Y-P, Lewis RNAH, Hodges RS, McElhaney RN (1992a) FTIR spectroscopic studies of the conformation and amide hydrogen exchange of a peptide model of the hydrophobic transmembrane α-helices of membrane proteins. Biochemistry 31:11572–11578

Zhang Y-P, Lewis RNAH, Hodges RS, McElhaney RN (1992b) Interaction of a peptide model of a hydrophobic transmembrane α-helical segment of a membrane protein with phosphatidylcholine bilayers: differential scanning calorimetric and FTIR spectroscopic studies. Biochemistry 31:11579–11588